

Fe/ZSM-5-Catalyzed-Synthesis of 1,4-Dihydropyridines under Ultrasound Irradiation and Their Antioxidant Activities

(Fe/ZSM-5-Pemangkin-Sintesis 1,4-Dihidropiridin di Bawah Sinaran Ultrabunyi dan Aktiviti Antioksidannya)

YAYAN DWI SUTARNI, BAMBANG PURWONO, EKO SRI KUNARTI & MUHAMMAD IDHAM DARUSSALAM MARDJAN*

Department of Chemistry, Faculty of Mathematics and Natural Sciences, Universitas Gadjah Mada, Yogyakarta 55281, Indonesia

Received: 24 July 2022/Accepted: 26 February 2023

ABSTRACT

A small library of 1,4-dihydropyridines have been synthesized from ethyl acetoacetate, ammonium acetate and various aldehydes via Hantzsch multicomponent reaction in the presence of Fe/ZSM-5 catalyst under ultrasound irradiation for 90 min. 1,4-Dihydropyridine derivatives were obtained in 64-86% yields and the heterogeneous Fe/ZSM-5 catalyst can be employed for four reaction cycles without losing the catalytic activity. All products were evaluated for their antioxidant activities using the DPPH method and compound **4g** was found to be an effective antioxidant agent with DPPH activity of 83.5%.

Keywords: Antioxidant assay; Fe/ZSM-5 catalyst; ultrasound-assisted-multicomponent reaction; 1,4-dihydropyridines

ABSTRAK

Terbitan 1,4-dihidropiridin telah disintesis daripada etil asetoasetat, ammonium asetat dan pelbagai aldehid melalui tindak balas pelbagai komponen Hantzsch yang dimungkinkan oleh Fe/ZSM-5 di bawah penyinaran ultrabunyi selama 90 minit. Terbitan 1,4-dihidropiridin diperolehi dengan hasil 64-86% dan mangkin heterogen Fe/ZSM-5 boleh digunakan untuk 4 kitaran tindak balas tanpa kehilangan aktiviti pemangkin. Semua produk telah dinilai untuk aktiviti antioksidannya menggunakan kaedah DPPH dan sebatian **4g** didapati sebagai agen antioksidan yang berkesan dengan aktiviti DPPH sebesar 83.5%.

Kata kunci: Pemangkin Fe/ZSM-5; tindak balas pelbagai komponen dibantu ultrabunyi; ujian antioksidan; 1,4-dihidropiridin

INTRODUCTION

1,4-dihydropyridines are the prevalent nitrogen heterocycles found in the field of pharmacology. These moieties are widely utilized as calcium channel blockers (CBs) for the treatment of hypertension and cardiac diseases. Amlodipine, nifedipine, and nifedipine are representatives of CBs drugs bearing 1,4-dihydropyridine scaffolds (Ioan et al. 2011). In addition, 1,4-dihydropyridines display biological activities as antioxidant (Cahyana et al. 2020), anti-inflammatory (Samaunnisa et al. 2013), and antituberculosis (Manvar et al. 2010). The very promising

biological activities of 1,4-dihydropyridines encourage researchers to develop efficient synthetic strategies to access these heterocycles.

One of the strategies to prepare 1,4-dihydropyridines can be carried out through pyridine dearomatization (Heusler et al. 2021). However, the dearomatization process were not selective, reversible and requires extreme conditions. Hence, it prompted researchers to develop the synthesis of 1,4-dihydropyridines through multicomponent reaction involving aldehydes, dicarbonyl compounds, and ammonia in alcohol solvent under reflux (Patil et al. 2014). The application of this

multicomponent reaction has been directed to meet the Green Chemistry Principles, i.e., by employing catalysts to accelerate the reaction (Alponti et al. 2021).

Various homogeneous catalysts, such as ascorbic acid (Sehout et al. 2017), and citric acid (Patil et al. 2019), have been applied in the synthesis of 1,4-dihydropyridines. However, these catalysts were difficult to separate from the products and could not be reused for the subsequent process. To address these problems, 1,4-dihydropyridines have been synthesized in the presence of heterogeneous catalysts, including silica boron sulphuric acid nanoparticles (SBASNs (Khalafi-Nezhad et al. 2013)), sulfuric acid modified by polyethylene glycol (PEG-OSO₃H (Vekariya & Patel 2015)) and cellulose matrix embedded copper decorated magnetic bionanocomposite (γ -Fe₂O₃/Cu@cellulose (Maleki et al. 2019)).

Zeolites are other potential heterogeneous catalysts that can be used to synthesize 1,4-dihydropyridines. Several types of zeolites have been used in 1,4-dihydropyridine synthesis including HY-zeolite (Nikpassand, Mamaghani & Tabatabaieian 2009) and USY-zeolite (Alponti et al. 2021) under reflux in ethanol. In many organic processes, zeolites have been widely reported to be selective and efficient catalysts since their acidity and porosity are easily controlled and modified (Ennaert et al. 2016). For example, metals can be impregnated to zeolite framework to increase their activity and selectivity (Wang et al. 2019). Metals, such as Zr (Kusampally et al. 2020), Cu (Tursunov, Kustov & Tilyabaev 2019), Fe (Mohammed et al. 2020), and Ni (Huynh et al. 2014) can be loaded into zeolite structure to increase its activity and selectivity. Zeolite ZSM-5 has been widely employed in various type of reaction due to its hydrothermal stability, well-structured pore as well as high surface area.

In some cases, performing the synthesis of 1,4-dihydropyridines in the presence of metal-anchored-catalysts may take long reaction time (Oskuie et al. 2020). Sonochemical method using ultrasound irradiation has emerged a green method which is easily controlled and energy efficient which allows the organic reactions to take place in short reaction time with good reaction yields and selectivity (Sancheti & Gogate 2017). Numbers of 1,4-dihydropyridine derivatives have been efficiently generated in the presence of supported ionic liquid phase (SILP) catalyst (Jagadale et al. 2018) and nanocomposite hybrid catalyst derived from cellulose matrix and volcanic pumice (Valadi et al. 2020).

In this study, we demonstrate the preparation and application of Fe/ZSM-5 catalyst in the synthesis of 1,4-dihydropyridines from ethyl acetoacetate, ammonium acetate and various aldehydes under ultrasound irradiation. In addition, the reusability of the heterogeneous catalyst and antioxidant activity of the products are also investigated.

MATERIALS AND METHODS

Shandong Nanotechnology provided the zeolite (NH₄-ZSM-5). Materials such as Fe(NO₃)₂·9H₂O, ethyl acetoacetate, ammonium acetate, variety of aldehydes (benzaldehyde, 4-methoxybenzaldehyde, 4-methylbenzaldehyde, 4-bromobenzaldehyde, 4-chlorobenzaldehyde, paraformaldehyde, and furfural), ethanol, *n*-hexane, ethyl acetate 25% and ammonium solution were purchased from Merck. The X-Ray Diffraction (XRD) pattern of catalysts was obtained from XRD (*Shimadzu XRD Lab-X600*) between 5 and 90° (2 θ) with Cu K α radiation ($\lambda = 1.5418 \text{ \AA}$). The morphology and metal content on the surface of catalysts were determined by scanning electron microscope with energy dispersive X-Ray spectroscopy (SEM-EDX, *JEOL JSM-6510LA*). The pore size of catalysts was determined by *Surface Area Analyzer* (SAA, The Gemini VII 2037 series). Synthesis of 1,4-dihydropyridines was carried out in an ultrasound bath *Power sonic 505* (40 kHz and 350 watt). The pure products were elucidated using Fourier Transform Infrared Spectrometer (FTIR, *Shimadzu Prestige 21*) in KBr pellet, Gas Chromatography-Mass Spectrometer (GC-MS, *GCMS-QP2010S SHIMADZU*) and Nuclear Magnetic Resonance Spectrometer (NMR, *JNM-ECZ500R* 500 MHz for ¹H-NMR and 125 MHz for ¹³C-NMR) using CDCl₃ as solvent (δ 7.26 ppm) and tetramethylsilane (TMS) as reference. Chemical shifts were measured in parts per million (ppm) and coupling constants (*J*) were measured in Hertz (Hz). The TLC Silica gel 60 G F₂₅₄ was used and visualized using UV Light (254 nm). The melting point apparatus (*Stuart R000100898*) was used to determine the melting points without any correction.

PREPARATION AND CHARACTERIZATION OF CATALYST

Catalyst preparation was carried out through wet impregnation according to previous study (Kostyniuk, Key & Mdleleni 2020), with slight modification. Zeolite NH₄-ZSM-5 (10 g) was dried at 120 °C for 12 h, then calcined with air flow for 5 h at 550 °C to give

H-ZSM-5. As much as of 0.404 g of metal salt precursor of $\text{Fe}(\text{NO}_3)_3 \cdot 9\text{H}_2\text{O}$ was dissolved in 100 mL deionized water to get 0.01 M of salt solution. Then, 10 g of H-ZSM-5 was mixed to the metal salt solution in 200 rpm stirring at 90 °C for 3 h. Thereafter, solid was dried at 120 °C overnight and calcined at 550 °C for 6 h. The catalyst Fe/ZSM-5 was crushed into 250-400 μm particle size and passed through 40 mesh sieves. The catalyst was characterized by FTIR, XRD, BET, and SEM-EDX.

GENERAL PROCEDURE FOR SYNTHESIS OF 1,4-Dihydropyridines

Ethyl acetoacetate (2.5 mmol, 0.33 mL, 2.5 equiv.), aldehydes (1.0 mmol, 1 equiv.), ammonium acetate (1.5 mL, 0.12 g, 1.5 equiv.), Fe/ZSM-5 (30 mg) and 3 mL of ethanol were subsequently introduced into 25 mL of flask. The reaction was carried out at 50 °C for 1.5 h under ultrasound irradiation. The reaction mixture was then cooled to room temperature. Ethanol (5 mL) was added to the reaction mixture, and it was centrifuged to separate the catalyst. The reaction mixture was dried with sodium sulphate, filtered and evaporated under reduced pressure. The crude product was purified by either recrystallization (from hot ethanol) or column chromatography (eluent of *n*-hexane and ethyl acetate of the ratio 8:2). The product was elucidated by means of ^1H NMR, ^{13}C NMR, FTIR, and GC-MS spectrometers.

Diethyl 4-(phenyl)-2,6-dimethyl-1,4-dihydropyridine-3,5-dicarboxylate (**4a**) (Kusampally et al. 2020). Following the general procedure for synthesis of 1,4-dihydropyridines using ethyl acetoacetate (2.5 mmol, 0.33 mL, 2.5 equiv.), benzaldehyde (1.0 mmol, 0.1 mL, 1 equiv.), ammonium acetate (1.5 mL, 0.12 g), Fe/ZSM-5 (30 mg) produced the desired compound **4a**. Yellow solid, m.p. 156-158 °C; EI/MS (*m/z*): 329; FTIR (KBr: ν , cm^{-1}): 3340, 3240, 2978, 1689, 1489, 1303, 1211; ^1H -NMR (500 MHz, CDCl_3 , δ , ppm) 7.27 (d, $J = 8.1$ Hz, 2H), 7.18 (t, $J = 8.1$ Hz, 2H), 7.12-7.09 (m, 1H), 5.62 (s, 1H), 4.98 (s, 1H), 4.11-4.04 (m, 4H), 2.32 (s, 6H), 1.21 (t, $J = 7.1$ Hz, 6H); ^{13}C -NMR (125 MHz, CDCl_3 , δ , ppm) 167.8, 147.9, 128.1, 128.0, 126.2, 104.3, 59.9, 39.7, 19.7, 14.4.

Diethyl 2,6-dimethyl-4-(*p*-tolyl)-1,4-dihydropyridine-3,5-dicarboxylate (**4b**) (Niaz et al. 2015). Following the general procedure for synthesis of 1,4-dihydropyridines using ethyl acetoacetate (2.5 mmol, 0.33 mL, 2.5 equiv.), 4-methylbenzaldehyde (1.0 mmol, 0.12 mL, 1 equiv.), ammonium acetate (1.5

mL, 0.12 g), Fe/ZSM-5 (30 mg) produced the desired compound **4b**. Light yellow powder, m.p. 130-132 °C; EI/MS (*m/z*): 343; FTIR (KBr: ν , cm^{-1}): 3302, 3093, 2987, 1689, 1496, 1203, 1103; ^1H -NMR (500 MHz, CDCl_3 , δ , ppm) 7.17 (d, $J = 8.1$ Hz, 2H), 7.01 (d, $J = 8.1$ Hz, 2H), 5.55 (s, 1H), 4.95 (s, 1H), 4.11-4.07 (m, 4H), 2.32 (s, 3H), 2.27 (s, 6H), 1.21 (t, $J = 7.1$ Hz, 6H); ^{13}C -NMR (125 MHz, CDCl_3 , δ , ppm) 167.5, 144.7, 143.5, 135.4, 128.5, 127.7, 104.2, 59.6, 39.0, 20.9, 19.5, 14.1.

Diethyl 4-(4-methoxyphenyl)-2,6-dimethyl-1,4-dihydropyridine-3,5-dicarboxylate (**4c**) (Srinivasan, Pachamutu & Maheswari 2019). Following the general procedure for synthesis of 1,4-dihydropyridines using ethyl acetoacetate (2.5 mmol, 0.33 mL, 2.5 equiv.), 4-methoxybenzaldehyde (1.0 mmol, 0.12 mL, 1 equiv.), ammonium acetate (1.5 mL, 0.12 g), Fe/ZSM-5 (30 mg) produced the desired compound **4c**. Yellow solid, m.p. 160-161 °C; EI/MS (*m/z*): 359; FTIR (KBr: ν , cm^{-1}): 3340, 3093, 2997, 1689, 1489, 1303, 1211; ^1H -NMR (500 MHz, CDCl_3 , δ , ppm) 7.19 (d, $J = 8.7$ Hz, 2H), 6.75 (d, $J = 8.7$ Hz, 2H), 5.67 (s, 1H), 4.92 (s, 1H), 4.12-4.05 (m, 4H), 3.75 (s, 3H), 2.31 (s, 6H), 1.22 (t, $J = 7.1$ Hz, 6H); ^{13}C -NMR (125 MHz, CDCl_3 , δ , ppm) 167.6, 157.7, 143.5, 140.2, 128.8, 113.1, 104.2, 59.6, 55.0, 38.6, 19.5, 14.1.

Diethyl 4-(4-bromophenyl)-2,6-dimethyl-1,4-dihydropyridine-3,5-dicarboxylate (**4d**) (Srinivasan, Pachamutu & Maheswari 2019). Following the general procedure for synthesis of 1,4-dihydropyridines using ethyl acetoacetate (2.5 mmol, 0.33 mL, 2.5 equiv.), 4-bromobenzaldehyde (1.0 mmol, 184 mg, 1 equiv.), ammonium acetate (1.5 mL, 0.12 g), Fe/ZSM-5 (30 mg) produced the desired compound **4d**. Light yellow solid, m.p. 159-160 °C; EI/MS (*m/z*): 407; FTIR (KBr: ν , cm^{-1}): 3356, 3093, 2987, 1689, 1489, 1373, 1203, 1095; ^1H -NMR (500 MHz, CDCl_3 , δ , ppm) 7.33 (d, $J = 8.4$ Hz, 2H), 7.16 (d, $J = 8.4$ Hz, 2H), 5.59 (s, 1H), 4.94 (s, 1H), 4.12-4.05 (m, 4H), 2.33 (s, 6H), 1.22 (t, $J = 7.2$ Hz, 6H); ^{13}C -NMR (125 MHz, CDCl_3 , δ , ppm) 167.5, 147.0, 144.1, 131.0, 130.0, 120.0, 104.0, 60.0, 39.5, 19.8, 14.4.

Diethyl 4-(4-chlorophenyl)-2,6-dimethyl-1,4-dihydropyridine-3,5-dicarboxylate (**4e**) (Niaz et al. 2015). Following the general procedure for synthesis of 1,4-dihydropyridines using ethyl acetoacetate (2.5 mmol, 0.33 mL, 2.5 equiv.), 4-chlorobenzaldehyde (1.0 mmol, 140 mg, 1 equiv.), ammonium acetate (1.5 mL, 0.12 g), Fe/ZSM-5 (30 mg) produced the desired compound **4e**. Yellow solid, m.p. 147-150 °C; EI/MS (*m/z*): 363; FTIR (KBr: ν , cm^{-1}): 3356, 3093, 2985, 1689, 1489, 1373, 1211, 1095; ^1H -NMR (500 MHz, CDCl_3 , δ , ppm) 7.10 (d, $J = 8.5$

Hz, 2H), 7.05 (d, $J = 8.5$ Hz, 2H), 4.85 (s, 1H), 4.70 (s, 1H), 4.04-3.93 (m, 4H), 2.28 (s, 6H), 1.12 (t, $J = 7.1$ Hz, 6H); $^{13}\text{C-NMR}$ (125 MHz, CDCl_3 , δ , ppm) 167.6, 146.5, 144.1, 129.6, 128.1, 127.9, 104.1, 60.0, 39.4, 19.8, 14.4.

Diethyl 4-(furan-2-yl)-2,6-dimethyl-1,4-dihydropyridine-3,5-dicarboxylate (**4f**) (Niaz et al. 2015). Following the general procedure for synthesis of 1,4-dihydropyridines using ethyl acetoacetate (2.5 mmol, 0.33 mL, 2.5 equiv.), furfural (1.0 mmol, 0.09 mL, 1 equiv.), ammonium acetate (1.5 mL, 0.12 g), Fe/ZSM-5 (30 mg) produced the desired compound **4f**. Light brown powder, m.p. 159-161 °C; EI/MS (m/z): 319; FTIR (KBr: ν , cm^{-1}): 3348, 3093, 2985, 1697, 1489, 1373, 1203, 1103; $^1\text{H-NMR}$ (500 MHz, CDCl_3 , δ , ppm) 7.20-7.19 (m, 1H), 6.20-6.19 (m, 1H), 5.93-5.92 (m, 1H), 5.69 (s, 1H), 5.19 (s, 1H), 4.21-4.09 (m, 4H), 2.32 (s, 6H), 1.25 (t, $J = 7.1$ Hz, 6H); $^{13}\text{C-NMR}$ (125 MHz, CDCl_3 , δ , ppm) 167.6, 158.8, 145.1, 141.0, 110.1, 104.6, 101.0, 60.0, 33.6, 19.7, 14.4.

Diethyl 2,6-dimethyl-1,4-dihydropyridine-3,5-dicarboxylate (**4g**) (Abdel-Mohsen, Conrad & Beifuss 2012). Following the general procedure for synthesis of 1,4-dihydropyridines using ethyl acetoacetate (2.5 mmol, 0.33 mL, 2.5 equiv.), paraformaldehyde (1.0 mmol, 30 mg, 1 equiv.), ammonium acetate (1.5 mL, 0.12 g), Fe/ZSM-5 (30 mg) produced the desired compound **4g**. Light yellow powder, m.p. 178-180 °C; EI/MS (m/z): 252; FTIR (KBr: ν , cm^{-1}): 3348, 2987, 1651, 1504, 1373, 1306, 1211; $^1\text{H-NMR}$ (500 MHz, CDCl_3 , δ , ppm) 8.66 (s, 1H), 4.40-4.36 (m, 4H), 3.24 (s, 2H), 2.83 (s, 6H), 1.27 (t, $J = 7.1$ Hz, 6H); $^{13}\text{C-NMR}$ (125 MHz, CDCl_3 , δ , ppm) 166.4, 145.2, 99.9, 61.9, 25.2, 19.6, 14.7.

REUSABILITY TEST OF Fe/ZSM-5 CATALYST

Having separated from the reaction mixture through the centrifugation process, Fe/ZSM-5 catalyst was centrifuged (washed) using ethanol (5 mL) for 5 min for 5 times. The catalyst was dried at 120 °C in an oven to remove ethanol. The recovered catalyst was then reused in the next cycle of ultrasound-assisted-synthesis of 1,4-dihydropyridines until significant reduction of reaction yield was observed.

ANTIOXIDANT ACTIVITIES

The free radical scavenging activity of 1,4-dihydropyridines (**4a-g**) was based on the stable DPPH radical scavenging activity according to Cahyana et al. (2020). In a separate tube, each 1 mL of 100 mg/mL of sample and BHT standard (positive control) solution in

methanol were placed. Then, 3 mL of freshly prepared 0.1 mM DPPH solution was added to the tube. The mixture was vortexed thoroughly and allowed to stand for 30 min in the dark condition. The absorbance of stable DPPH was measured at 517 nm. The same procedure was used to make a DPPH control test (sample was not included). The scavenging activity was calculated using the DPPH radical scavenging activity equation (Equation 1) and expressed as the inhibition rate in percent. A_{control} is the absorbance of the control solution, whereas A_{sample} is the absorbance of the sample.

$$\text{DPPH radical scavenging activity (\%)} = \frac{A_{\text{Control}} - A_{\text{Sample}}}{A_{\text{Control}}} \times 100 \quad (1)$$

RESULTS AND DISCUSSION

PREPARATION AND CHARACTERIZATION OF Fe/ZSM-5 CATALYST

Preparation of Fe/ZSM-5 catalyst was started by drying the commercial ZSM-5 at 120 °C to remove water. The catalyst was then calcined at 550 °C to eliminate ammonium ion and to give H/ZSM-5. The impregnation of metal into the zeolite framework was carried out through wet impregnation method by refluxing H/ZSM-5 with 0.01 M solution of $\text{Fe}(\text{NO}_3)_3 \cdot 9\text{H}_2\text{O}$. Further calcination at 550 °C was carried out to produce Fe/ZSM-5 in 98% yield. The H/ZSM-5 and Fe/ZSM-5 catalysts were characterized by SEM-EDX, XRD, FTIR, Brunauer Emmet Teller (BET) method for pore analysis using SAA, and acidity tests using gravimetry technique.

Analysis using SEM-EDX was conducted to determine the morphology and the presence of Fe on the surface of ZSM-5 after the impregnation. As displayed in Table 1, the existence of Fe on ZSM-5 framework indicates that the loading of Fe has taken place. The effect of metal impregnation to the morphology of catalyst can be seen in Figure 1. While H/ZSM-5 has the homogeneous structure, the surface of Fe/ZSM-5 is more heterogeneous and agglomerated. The morphology of ZSM-5 is irregular granular particles (Mohammed et al. 2020; Tursunov, Kustov & Tilyabaev 2019). The presence of metal impregnation does not change the morphology of ZSM-5 but leads the particles to easily agglomerate.

The characteristic XRD peaks of ZSM-5 are at 20 7.5-9.5° and 22-25° (JCPDS No. 42-0024). These peaks are present both in H/ZSM-5 and Fe/ZSM-5 indicating that the impregnation of metal does not affect the

crystallinity of ZSM-5 (Figure 2). The peaks of metal oxide are not observed at the diffractogram of Fe/ZSM-5 catalyst, suggesting that iron is dispersed on the surface of the unmodified catalyst H/ZSM-5 (Tursunov, Kustov & Tilyabaev 2019).

The FTIR spectrum of ZSM-5 will exhibit characteristic peaks at wavenumbers of 1220, 1075, 797, 542, and 433 cm^{-1} (Kostyniuk et al. 2020). Figure 3 shows that all ZSM-5 catalysts give absorption at the characteristic wavenumbers. The peaks at wavenumbers of 1075 and 797 cm^{-1} are asymmetric and symmetric

stretching vibrations originating from metal bonding with oxygen (T-O) in the internal structure of ZSM-5. The peaks at 433 and 542 cm^{-1} also demonstrate the stretching vibration of metal bond impregnated into ZSM-5 with oxygen in the ZSM-5 structure (Mohammed et al. 2020). The appearance of these peaks indicates that the metal impregnation has been successfully carried out. The two peaks at 1220 and 542 cm^{-1} are caused by the external asymmetric stretching vibration and the internal Si-O and Al-O tetrahedral bending vibrations in ZSM-5 double five rings (D5R) (Rahman et al. 2018).

TABLE 1. Element composition in the surface of ZSM-5 catalysts (% w/w)

Catalyst	Element (%)			
	Fe	O	Si	Al
H/ZSM-5	-	-	96,45	3,55
Fe/ZSM-5	0,35	51,93	38,02	1,47

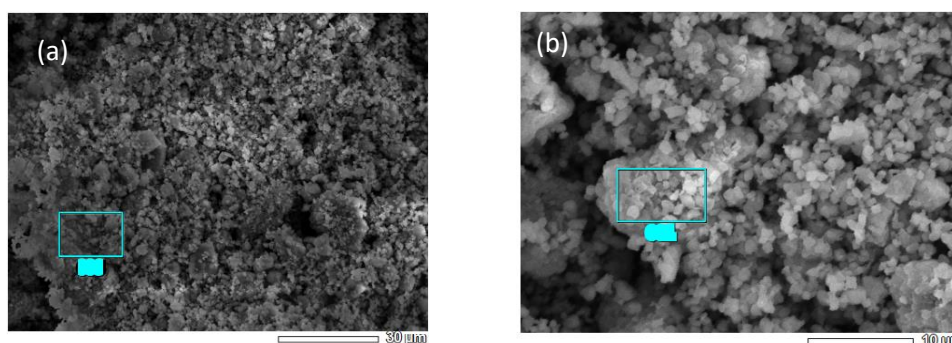


FIGURE 1. Morphology of catalysts: (a) H-ZSM-5 (b) Fe/ZSM-5

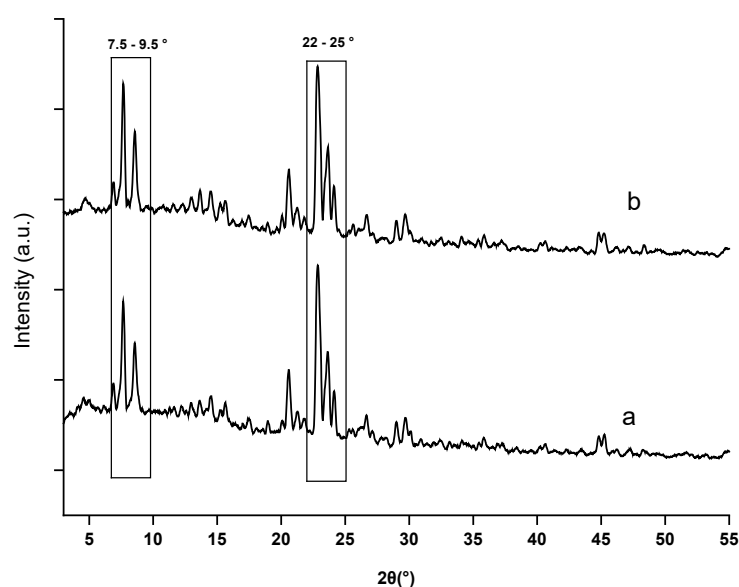


FIGURE 2. Diffractogram of catalysts: (a) H/ZSM-5 (b) Fe/ZSM-5

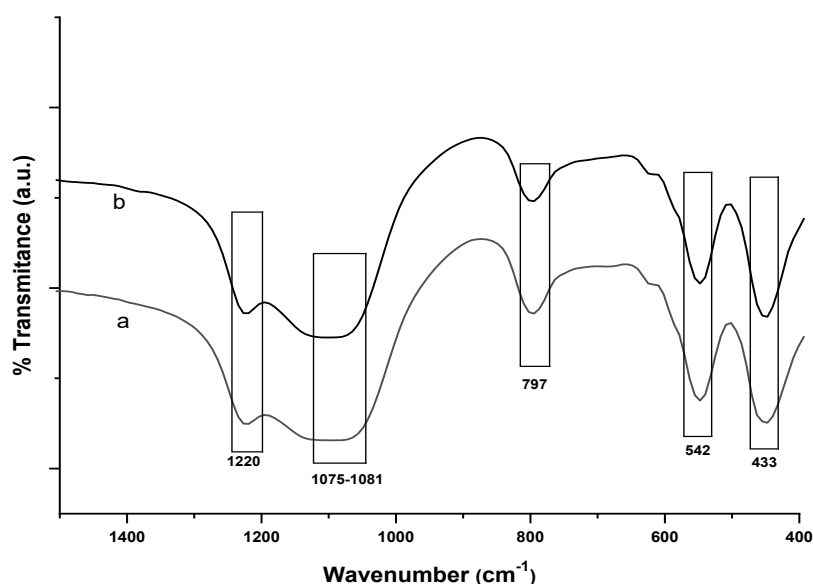


FIGURE 3. FTIR spectra of catalysts: (a) H/ZSM-5 (b) Fe/ZSM-5

The FTIR spectra (Figure 4) are also used to determine the presence of Brønsted and Lewis acid sites in the catalyst structure after adsorption with ammonia. The distinctive bands of Brønsted acid sites appear in the region of 1400 cm^{-1} , while the Lewis acid properties appear in the region of 1700 cm^{-1} (Niwa & Katada 2013). Furthermore, the characteristics of Brønsted acid derived from Si-OH-Al can be observed in the range of $3500\text{--}3700$. The existence of Brønsted acid sites, which are typical OH absorptions of Si-OH-Al in the five-membered ring of ZSM-5, is shown by the bands at 3752 and 3654 cm^{-1} . The presence of Lewis acid sites is then suggested by the peak at 1722 cm^{-1} . This peak is caused by the coordination between iron ion and ammonia. The appearance of bands at 3119 and 1397 cm^{-1} , corresponding to the stretching and bending vibrations of the N-H bond on the NH_4^+ ions that had been adsorbed by the catalyst, confirmed the presence of these two acids sites. The results of the total acidity from gravimetric ammonia adsorption show that the metal impregnation can increase the acidity of ZSM-5 catalyst (Table 2).

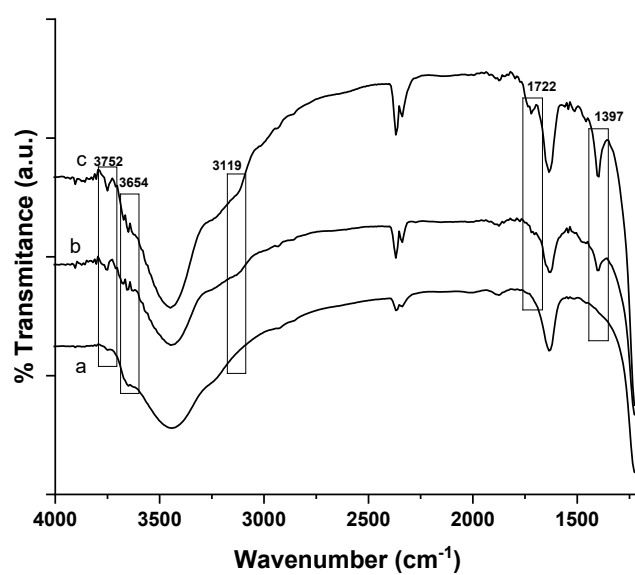
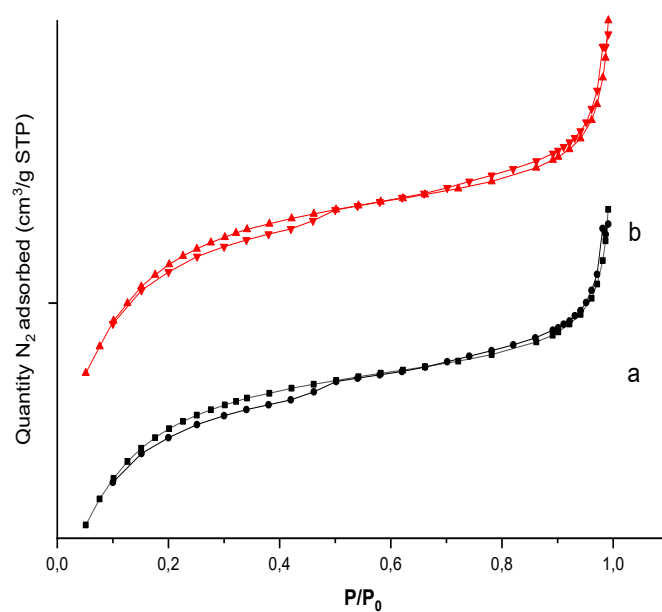
To determine the effect of metal impregnation on the surface area, volume, and pore diameter of the ZSM-5, pore analysis was carried out using BET method. The results of BET analysis are presented in Table 3. The N_2 adsorption-desorption isotherm in Figure 5 shows that the ZSM-5 catalysts have the type IV isotherm which is a characteristic of mesoporous materials. Based on Table 3, the addition of metal into ZSM-5 increases the BET surface area and total pore volume. The t-Plot method shows that the addition of metal decreases the micro surface area and micropore volume of the catalyst. This is probably because the metal is distributed unevenly which causes the pores to be covered by metal accumulation, and the surface area and pore volume decrease (Purnamasari et al. 2017). Figure 6 displays the metal-embedded zeolite pore size distribution. After metal impregnation, the distribution of zeolite pores changed to become microporous (pore volume $< 2\text{ nm}$). This is due to the ability of the metal ions to close the pores on ZSM-5 surface. The average pore diameter of the Fe impregnated zeolites increases since Fe ions will impregnate the zeolite surface and then gather to create new and larger pores.

TABLE 2. Total acidity of all catalysts (% w/w)

Elements (%)	Total acidity
H-ZSM-5	0.207
Fe-ZSM-5	0.275

TABLE 3. Results of BET analysis

Catalyst	Surface area (m ² /g)			Pore volume (cm ³ /g)		Pore diameter BJH (nm)
	BET	Langmuir	Micro (t-Plot)	Total	Micro (t-Plot)	
H/ZSM-5	318,167	507,734	223,240	0,202	0,125	4,155
Fe/ZSM-5	323,745	518,428	214,771	0,208	0,121	4,167

FIGURE 4. FTIR spectra of catalysts before: (a) H/ZSM-5; and after ammonia absorption (b) H/ZSM-5-NH₃ (c) Fe/ZSM-5-NH₃FIGURE 5. N₂ adsorption-desorption isotherm of catalysts: (a) H/ZSM-5 (b) Fe/ZSM-5

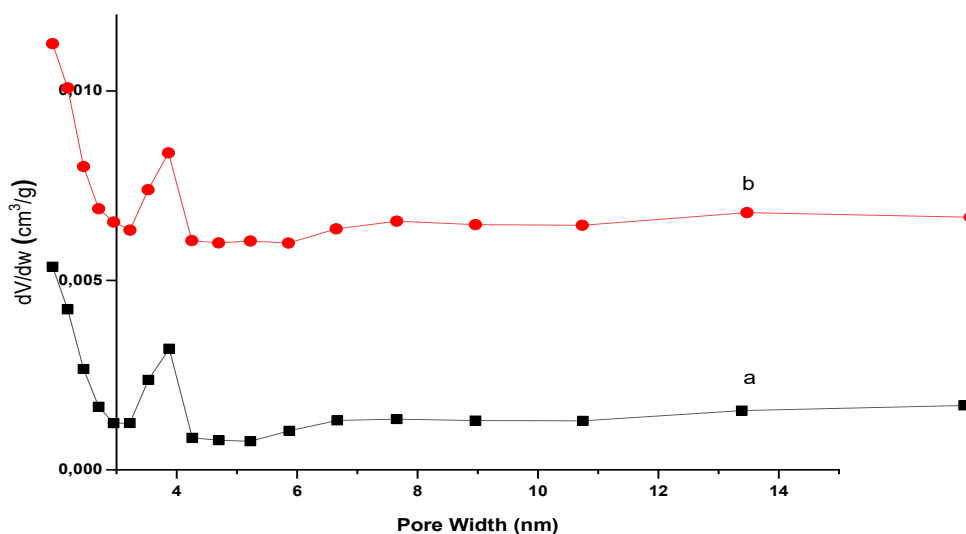


FIGURE 6. Pore size distribution: (a) H/ZSM-5 (b) Fe/ZSM-5

SYNTHESIS OF 1,4-dihydropyridines

The optimization of the multicomponent reaction for the synthesis of 1,4-dihydropyridine was carried out by employing the model substrates of ethyl acetoacetate **1**, benzaldehyde **2a**, and ammonium acetate **3** (Table 4). In the absence of Fe/ZSM-5 catalyst (Entry 1), the desired product is produced in 50% yield which is presumably due to the cavitation process produced by ultrasound irradiation which facilitates the collision process among the precursors (Draye, Estager & Kardos 2019). We are pleased to observe that performing the reaction in ethanol in the presence of 30 mg of Fe/ZSM-5 catalyst at 50 °C under ultrasound irradiation produces the desired product of diethyl 4-(phenyl)-2,6-dimethyl-1,4-dihydropyridine-3,5-dicarboxylate in 86% yield (Entry 2). We found that the solvent affects the catalytic performance of Fe/ZSM-5. While dichloromethane allows us to obtain the product in 78% yields, significant decrease in reaction yield is observed when we use acetonitrile as the solvent (Entries 3 and 4). The optimization of reaction temperature (Entries 2, 5 and 6) shows that the optimum temperature is 50 °C. The amount of catalyst was then optimized, where 10, 30, 50, and 100 mg of catalysts were used. The results shows that both decreasing (Entry 7) and increasing (Entries 8 and 9) decreases the catalytic performance of Fe/ZSM-5.

Several experiments were carried out to evaluate the performance of Fe/ZSM-5 for the synthesis of

1,4-dihydropyridine. The application of homogeneous catalyst of $\text{Fe}(\text{NO}_3)_3 \cdot 9\text{H}_2\text{O}$ salt gives the product in 60% yield (Entry 10). Even though the iron salt can act as catalyst in the synthesis of 1,4-dihydropyridine, this catalyst cannot be easily separated and reused. In addition, conducting the reaction in the presence of H/ZSM-5 catalyst allows us to obtain the product in 70% yield (Entry 11). The good catalytic performance of H/ZSM-5 is presumably due to the presence of both Brønsted and Lewis acid sites. The results showed that the metal impregnation may increase the available acid sites on the catalyst, allowing the synthesis of 1,4-dihydropyridines to rapidly proceed.

Having optimized the reaction conditions, the scope of ultrasound-assisted-synthesis of 1,4-dihydropyridines in the presence of low amount of Fe/ZSM-5 catalyst (Figure 7) has been evaluated. It should be noted that the multicomponent reaction was carried out under mild condition in short reaction time. In this study, various aldehydes were subjected to the reaction. The compatibility of aromatic aldehydes has been evaluated. The results shows that benzaldehydes bearing either electron donating- or withdrawing groups produces the corresponding 1,4-dihydropyridines (**4b-e**) in good yields. In addition, 1,4-dihydropyridines **4f** and **4g** are successfully generated from heterocyclic and aliphatic aldehydes, respectively. The results indicate that the structure and electronic properties of aldehydes does not affect the multicomponent reaction.

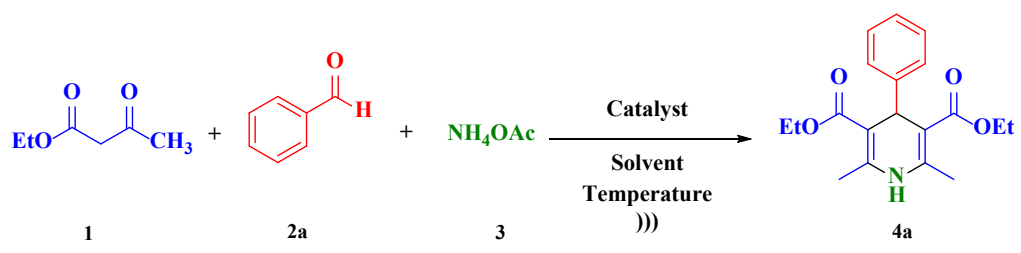
The synthesized 1,4-dihydropyridines were elucidated by $^1\text{H-NMR}$, $^{13}\text{C-NMR}$, FTIR and GCMS spectrometers. The formation of 1,4-dihydropyridine moiety is confirmed by the presence of methine proton (for **4a-f**) and methylene protons (for **4g**) at the region of 4.90-5.20 and 3.20-3.30 ppm, respectively. In addition, $^{13}\text{C-NMR}$ spectra exhibit two additional Csp^2 peaks (around 99-105 and 143-147 ppm) coming from 1,4-dihydropyridine ring. The FTIR spectra also show the absorbance at wavenumber of 3300-3360 cm^{-1} representing NH group of products. The GCMS analysis demonstrates that the products are obtained in good purity, where the obtained molecular mass is in full accordance with the mass of the desired products.

The proposed mechanism for the ultrasound-assisted-synthesis of 1,4-dihydropyridines catalyzed by Fe/ZSM-5 is depicted in Figure 8. This mechanism is similar with previous study by Allahresani et al. (2020). Initially, Fe/ZSM-5 catalyst will activate the carbonyl group of aldehydes **2** which will react with the enol form of ethyl acetoacetate **1** through a condensation reaction to produce intermediate **5**. The catalyst also interacts with dicarbonyl compound **1** and reacts with ammonia generated from ammonium acetate **3**

to form enamine **6**. The conjugate addition involving intermediates **5** and **6** generates species **7**, which in turn undergoes proton transfer and tautomerization to furnish aminoketones **9**. The subsequent intramolecular nucleophilic addition of amines to ketones **9** produces the desired 1,4-dihydropyridines **4**.

As heterogeneous catalysts, zeolites can be used for several cycles after being regenerated (Alponti et al. 2021). The regeneration of catalyst was carried out by washing the catalyst with ethanol to dissolve the organic compounds left. The physical treatment at 120 $^\circ\text{C}$ can vaporize water molecules that cover the acid sites, allowing the acid sites to be reactivated. The regenerated catalyst was then reused to produce 1,4-dihydropyridine derivative **4a** under the optimized conditions. According to Figure 9, the Fe/ZSM-5 catalyst can be reused up to four times without significantly reducing yield. After the fifth application, the reaction yield decreases to 50%, which is presumably due to the formation of coke from the organic compounds that are not depleted in the pores of the catalyst. Furthermore, the catalyst can be deactivated during the sintering via atomic migration, which is influenced by vibrations generated by ultrasound waves (Argyle & Bartholomew 2015).

TABLE 4. Optimization of ultrasound-assisted-towards the synthesis of 1,4-dihydropyridines



Entry	Catalysts	Solvent	Temperature ($^\circ\text{C}$)	Catalyst loading (mg)	Yield (%)
1	-	EtOH	50	-	50
2	Fe/ZSM-5	EtOH	50	30	86
3	Fe/ZSM-5	DCM	50	30	78
4	Fe/ZSM-5	MeCN	50	30	33
5	Fe/ZSM-5	EtOH	30	30	30
6	Fe/ZSM-5	EtOH	40	30	70
7	Fe/ZSM-5	EtOH	50	10	53
8	Fe/ZSM-5	EtOH	50	50	44
9	Fe/ZSM-5	EtOH	50	100	36
10	$\text{Fe}(\text{NO})_3 \cdot 9\text{H}_2\text{O}$	EtOH	50	30	60
11	H-ZSM-5	EtOH	50	30	70

DPPH RADICAL SCAVENGING ACTIVITY OF
1,4-dihydropyridines

The free radicals scavenging activity of 1,4-dihydropyridines **4a-g** was measured by DPPH assay according to Cahyana et al. (2020). The assay was carried out at the sample concentration of 100 μ M and used butylated hydroxytoluene (BHT) as the positive control. According to Figure 10, the DPPH activity of the unsubstituted 1,4-dihydropyridine **4a** is 24.5%. Introduction of both electron donating (Me **4b**, OMe **4c**) and withdrawing (Br **4d** and Cl **4e**) groups does not significantly affect the activity. Lower antioxidant

activity is observed when furanyl group **4f** is installed in the 1,4-dihydropyridine scaffold. Based on the DPPH assay, the presence of aromatic or heteroaromatic ring in 1,4-dihydropyridine moiety may destabilized the generated radicals resulting in low antioxidant activity. Among the synthesized 1,4-dihydropyridines, compound **4g** displays significant DPPH activity of 83.5% (>60%) presumably due to the presence of methylene group on 1,4-dihydropyridine ring. Despite the positive control (BHT) shows good antioxidant activity (92.1%), 1,4-dihydropyridine is still considered as an active antioxidant.

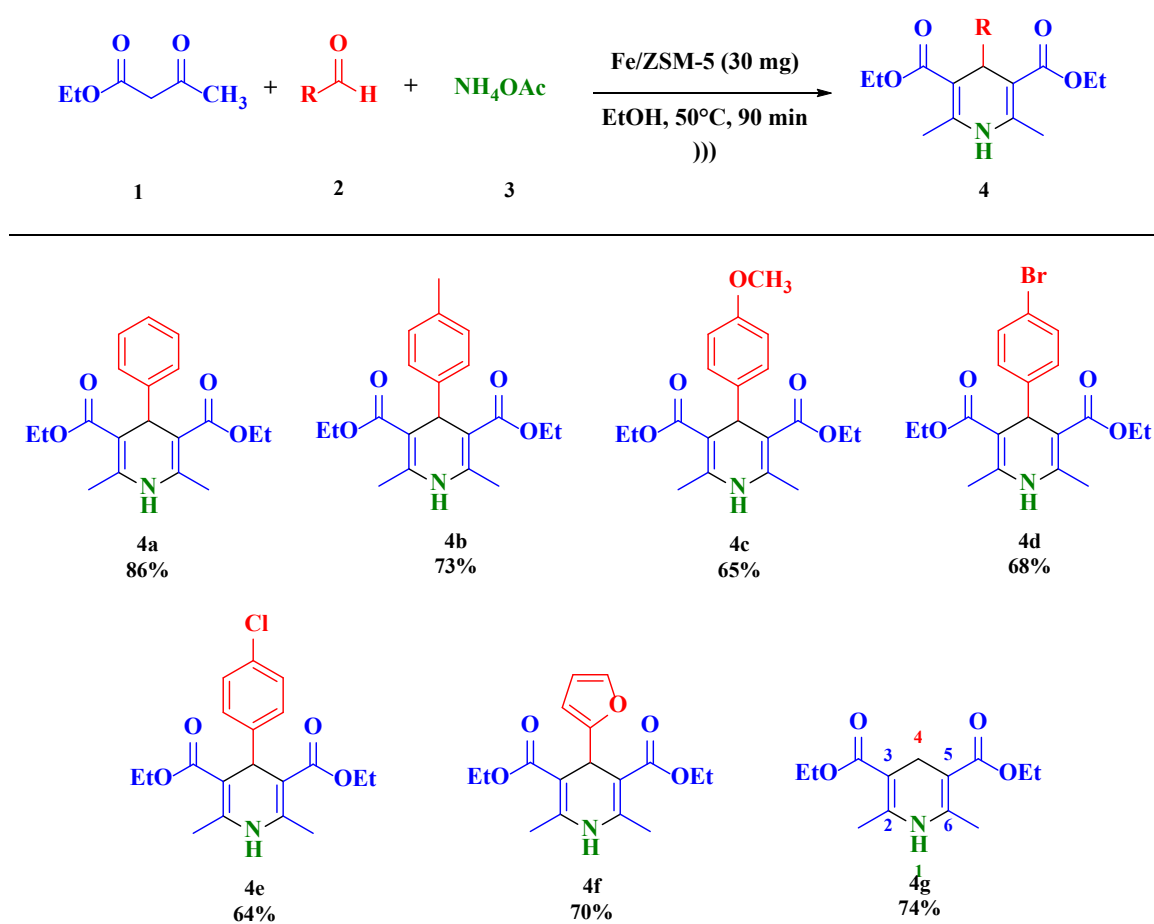


FIGURE 7. Scopes of ultrasound-assisted-synthesis of 1,4-dihydropyridines

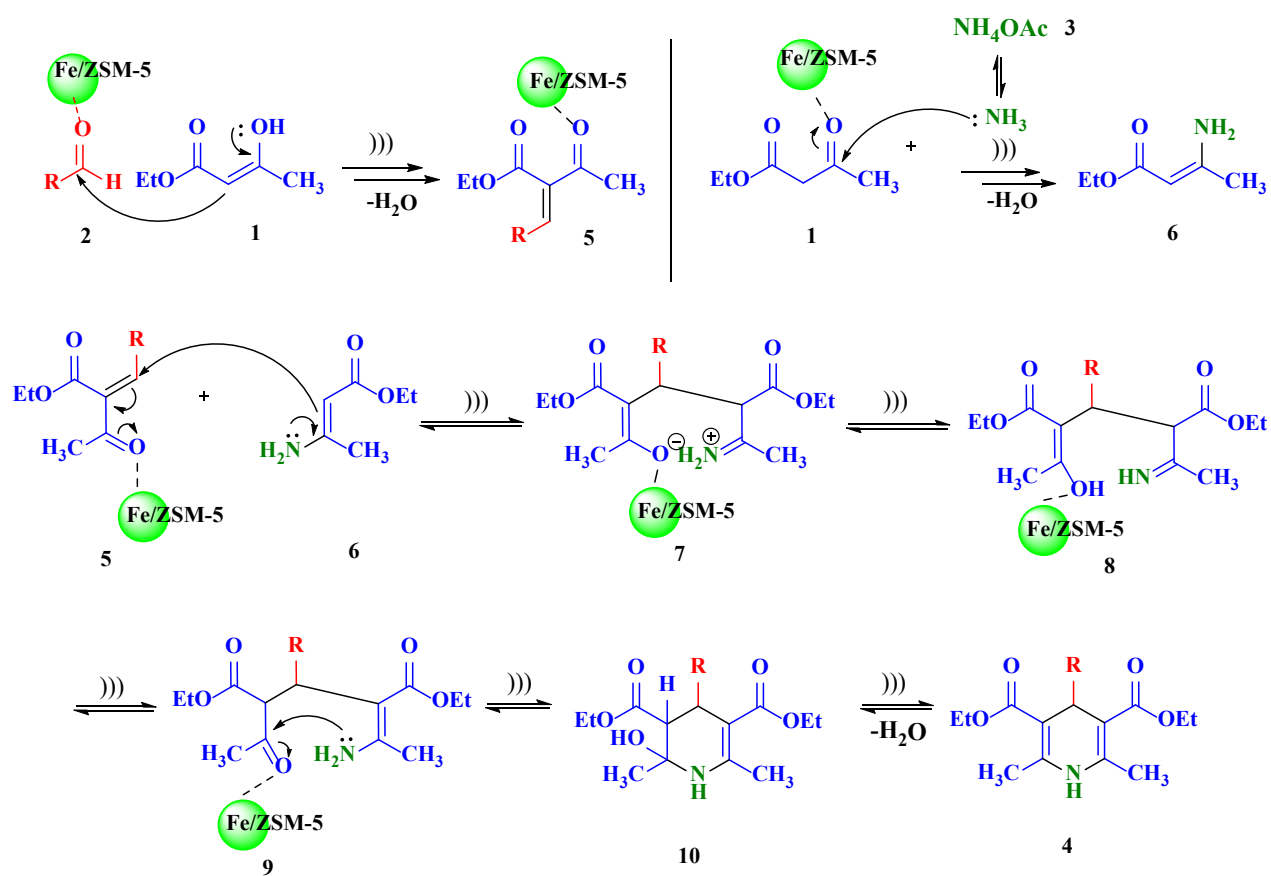


FIGURE 8. Proposed mechanism for the synthesis of 1,4-dihydropyridines using Fe/ZSM-5 catalyst under ultrasound irradiation

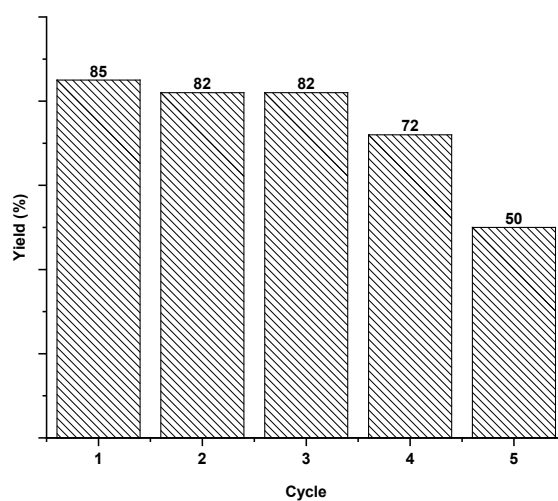


FIGURE 9. Reusability test of Fe/ZSM-5 catalyst for the synthesis of 1,4-dihydropyridines

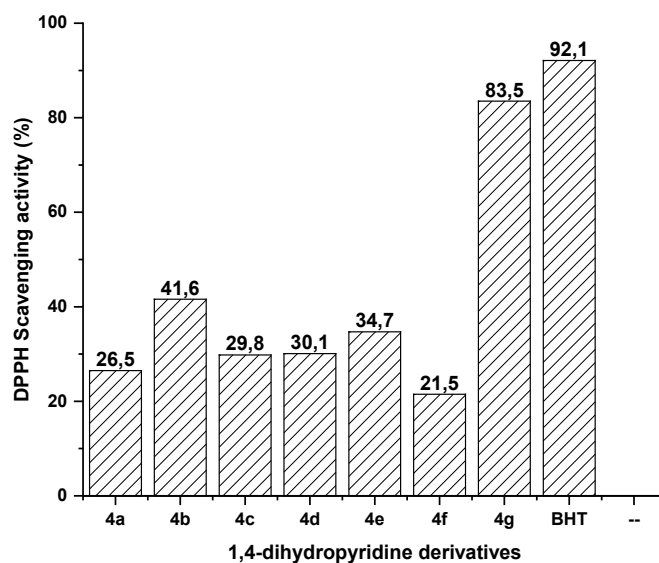


FIGURE 10. Antioxidant assay using DPPH radical scavenging activity of 1,4-dihydropyridines

CONCLUSION

To conclude, a convenient access to 1,4-dihydropyridines through Hantzsch multicomponent reaction in the presence of Fe/ZSM-5 catalyst under ultrasound irradiation have been developed. The desired products were obtained in good yields (up to 86%). The reusability test demonstrated that the heterogeneous catalyst can be reused for 4 catalytic cycles. The DPPH antioxidant assay showed that 1,4-dihydropyridine derivative **4g** (diethyl 2,6-dimethyl-1,4-dihydropyridine-3,5-dicarboxylate) showed promising biological activity with DPPH activity of 83.5%.

ACKNOWLEDGEMENTS

This work was financially supported by Dexa Group under Dexa Award Science Scholarship 2019. We would thank Universitas Gadjah Mada for the support through RTA program (5722/UN1.P.III/Dit-Lit/PT.01.05/2022). We acknowledge Prof. Endang Tri Wahyuni and Prof. Wega Tri Sunaryanti for the fruitful discussion.

REFERENCES

- Abdel-Mohsen, H.T., Conrad, J. & Beifuss, U. 2012. Laccase-catalyzed oxidation of Hantzsch 1,4-dihydropyridines to pyridines and a new one pot synthesis of pyridines. *Green Chem.* 14: 2686-2690.
- Allahresani, A., Sangani, M.M. & Nasser, M.A. 2020. CoFe₂O₄@SiO₂-NH₂-Co^{II} NPs catalyzed Hantzsch reaction as an efficient, reusable catalyst for the facile, green, one-pot synthesis of novel functionalized 1,4-dihydropyridine derivatives. *Appl. Organomet. Chem.* 34(9): e5759.
- Alponti, L.H.R., Picinini, M., Urquieta-Gonzalez, E.A. & Corrêa, A.G. 2021. USY-zeolite catalyzed synthesis of 1,4-dihydropyridines under microwave irradiation: Structure and recycling of the catalyst. *J. Mol. Struct.* 1227: 1-7.
- Arglye, M.D. & Bartholomew, C.H. 2015. Heterogeneous catalyst deactivation and regeneration: A review. *Catalysts* 5: 145-269.
- Cahyana, A.H., Liandi, A.R., Safitri, Y. & Yunarti, R.T. 2020. Synthesis of 1,4-dihydropyridine with aromatic of cinnamaldehyde compound using NiFe₂O₄ mnps catalyst and the activity test as antioxidant. *Rasayan J. Chem.* 13(3): 1491-1497.
- Draye, M., Estager, J. & Kardos, N. 2019. Organic sonochemistry: Ultrasound in green organic synthesis. In *Activation Methods Sonochemistry High Pressure*, Vol. 2, edited by Goddard, J-P., Malacria, M. & Ollivier, C. ISTE Ltd and John Wiley & Sons, Inc. 2019: 1-93.
- Ennaert, T., Aelst, J.V., Dijkmans, J., Clercq, R.D., Schutsyner, W., Dusselier, M., Verboekend, D. & Sels, B.F. 2016. Potential and challenges of zeolite chemistry in the catalytic conversion of biomass. *Chem. Soc. Rev.* 45: 584-611.
- Heusler, A., Fliege, J., Wagener, T. & Glorius, F. 2021. Substituted dihydropyridine synthesis by dearomatization of pyridines. *Angew. Chem. Int. Ed.* 60: 13793-13797.

- Hyunh, T.M., Armbruster, U., Pohl, M.M., Schneider, M., Radnik, J., Hoang, D., Phan, B.M.Q., Nguyen, D.A. & Martin, A. 2014. Hydrodeoxygenation of phenol as a model compound for bio-oil on non-noble bimetallic nickel-based catalysts. *Chem. Cat. Chem.* 6: 1940-1951.
- Ioan, P., Carosati, E., Micucci, M., Cruciani, G., Broccatelli, F., Zhoroz, B.S., Chairini, A. & Budriesi, R. 2011. 1,4-dihydropyridine scaffold in medicinal chemistry, the story so far and perspective (Part 1): Action in ion channels and GPCRs. *Curr. Med. Chem.* 18: 4901-4922.
- Jagadale, M., Kale, D., Salunkhe, R., Rajmane, M. & Rashinkar, G. 2018. Compatibility of supported ionic liquid phase catalysts under ultrasonication. *J. Mol. Liq.* 265: 525-535.
- Khalafi-Nezad, A., Panahi, F., Mohammadi, S. & Foroughi, H.O. 2013. A green and efficient procedure for one-pot synthesis of xanthenes and acridines using silica boron-sulfuric acid nanoparticles (SBSANs) as a solid Lewis-protic acid. *J. Iran Chem. Soc.* 10: 189-200.
- Kostyniuk, A., Key, D. & Mdleleni, M. 2020. 1-hexene isomerization over bimetallic M-Mo-ZSM-5 (M: Fe, Co, Ni) zeolite catalysts: Effects of transition metals addition on the catalytic performance. *J. Energy Inst.* 93: 552-564.
- Kusampally, U., Dhachapally, N., Kola, R. & Kamatala, C. 2020. Zeolite anchored Zr-ZSM-5 as an ecofriendly, green, and reusable catalyst in Hantzsch synthesis of dihydropyridine derivatives. *Mater. Chem. Phys.* 242: 1-8.
- Maleki, A., Eskandarpour, V., Rahimi, J. & Hamidi, N. 2019. Cellulose matrix embedded copper decorated magnetic bionanocomposite as a green catalyst in the synthesis of dihydropyridines and polyhydroquinolines. *Carbohydr. Polym.* 208: 251-260.
- Manvar, A.T., Pissurlenkar, R.R.S., Virsodia, V.R., Upadhyay, K.D., Manvar, D.R., Mishra, A.K., Acharya, H.D., Parecha, A.R., Dholakia, C.D., Shah, A.K. & Coutinho, E. 2010. Synthesis, *in-vitro* antitubercular activity and 3D-QSAR study of 1,4-dihydropyridines. *Mol. Divers.* 14: 285-305.
- Mohammed, B.B., Hsini, A., Abdellaoui, Y., Oualid, H.A., Laabd, M., Ouadi, M., Addi, A., Yamni, K. & Tijani, N. 2020. Fe-ZSM-5 zeolite for efficient removal of basic fuchsin dye from aqueous solutions: Synthesis, characterization and adsorption process optimization using BBD-RSM modelling. *J. Env. Chem. Eng.* 8: 1-11.
- Niaz, H., Kashtoh, H., Khan, J.A.J., Khan, A., Wahab, A., Alam, M.T., Khan, K.M., Perveen, S. & Choudhary, I. 2015. Synthesis of diethyl 4-substituted-2,6-dimethyl-1,4-dihydropyridine-3,5-dicarboxylates as a new series of inhibitors against yeast α -glucosidase. *Eur. J. Med. Chem.* 95: 199-209.
- Nikpassand, M., Mamaghani, M. & Tabatabaieian, K. 2009. An efficient one-pot three-component synthesis of fused 1,4-dihydropyridines using HY-Zeolite. *Molecules* 14: 1468-1474.
- Niwa, M. & Katada, N. 2013. New method for the temperature-programmed desorption (TPD) of ammonia experiment for characterization of zeolite acidity: A review. *Chem. Rec.* 13: 432-455.
- Oskuie, E.F., Azizi, S., Ghasemi, Z., Pirouzmand, M., Kojanag, B.N. & Soleymani, J. 2020. Zn/MCM-41-catalyzed unsymmetrical Hantzsch reaction and the evaluation of optical properties and anti-cancer activities of the polyhydroquinoline products. *Monatsh. Chem.* 151: 243-249.
- Patil, M., Karhale, S., Kudale, A., Kumbhar, A., More, S. & Helavi, V. 2019. Green protocol for the synthesis of 1,8-Dioxo-decahydroacridines by Hantzsch condensation using citric acid as organocatalyst. *Curr. Sci.* 116: 936-942.
- Patil, D., Chandam, D., Mulik, A., Patil, P., Jagadale, S., Kant, R., Gupta, V. & Deshmukh, M. 2014. Novel Brønsted acidic ionic liquid ([CMIM][CF₃COO]) prompted multicomponent Hantzsch reaction for the eco-friendly synthesis of acridinediones: An efficient and recyclable catalyst. *Catal. Lett.* 144: 949-958.
- Purnamasari, A.P., Sari, M.E.M., Kusumaningtyas, D.T., Suprpto, S., Hamid, A. & Prasetyoko, D. 2017. The effect of mesoporous H-ZSM-5 crystallinity as a CaO support on the transesterification of used cooking oil. *Bull. Chem. React.* 12: 329-336.
- Rahman, M.M., Abu-Zied, B.M. & Asiri, A.M. 2018. Cu-loaded ZSM-5 zeolites: An ultra-sensitive phenolic sensor development for environmental safety. *J. Ind. Eng. Chem.* 61: 304-313.
- Samaunnisa, A., Mohammed, R., Venkataramana, C.H.S. & Madhavan, V. 2013. Evaluation of 2,6-Dimethyl-N₃,N₅-diphenyl-1,4-dihydropyridine-3, 5-dicarbohydrazide derivatives for *in vivo* anti-inflammatory and analgesic activities. *Int. Res. J. Pharm.* 4(9): 156-159.
- Sancheti, S.V. & Gogate, P.R. 2017. A review of engineering aspects of intensification of chemical synthesis using ultrasound. *Ultrason. Sonochem.* 36: 527-543.
- Sehout, I., Boulcina, R., Boumoud, B., Boumoud, T. & Debache, A. 2017. Solvent-free synthesis of polyhydroquinoline and 1,8-dioxodecahydroacridine derivatives via the Hantzsch reaction catalyzed by a natural organic acid: A green method. *Synth. Comm.* 47: 1185-1191.
- Srinivasan, V.V., Pachamutu, M.P. & Maheswari, R. 2015. Lewis acidic mesoporous Fe-TUD-1 as catalysts for synthesis of Hantzsch 1,4-dihydropyridine derivatives. *J. Porous Mater.* 22: 1187-1194.
- Tursunov, O., Kustov, L. & Tilyabaev, Z. 2019. Catalytic activity of H-ZSM-5 and Cu-HZSM-5 zeolites of medium SiO₂/Al₂O₃ ratio in conversion of n-Hexane to aromatics. *J. Pet. Sci. Eng.* 180: 773-778.
- Valadi, K., Gharibi, S., Taheri-Ledari, R. & Maleki, A. 2020. Ultrasound-assisted synthesis of 1,4-Dihydropyridine derivatives by an efficient volcanic-based hybrid nanocomposite. *Solid State Sci.* 101: 1-7.

Vekariya, H. & Patel, H.D. 2015. Sulfonated polyethylene glycol (PEG-OSO₃H) as a polymer supported biodegradable and recyclable catalyst in green organic synthesis: Recent advances. *Chem. Soc. Rev.* 5: 49006-49030.

Wang, Q., Zhu, M., Zhang, H., Xu, C., Dai, B. & Zhang, J. 2019. Enhanced catalytic performance of Zr-ZSM-5-supported Zn for the hydration of acetaldehyde. *Catal. Commun.* 120: 33-37.

*Corresponding author; email: idham.darussalam@ugm.ac.id